Multifunctional Luminescent Material Based on Quinoxaline and Triphenylamine Groups: Polymorphism, Mechanochromic Luminescence, and Applications in High-efficiency Fluorescent OLED

Wen Zhengjie [a], Yang Tingting [b], Zhang Di [a], Wang Zhengqin [a], Dong Shufan [a], Xu Huixia [a*], Miao Yanqin [a*], Zhao Bo [a], Wang Hua [a]

[a] *Key Laboratory of Interface Science and Engineering in Advanced Materials, Ministry of Education, Taiyuan University of Technology, Taiyuan 030024, China.*

[b] *Shanxi Province Key Laboratory of Microstructure Functional Materials Institute of Solid State Physical, School of Physics and Electronic Science, Shanxi Datong University, Datong, 037009, China*

Supporting information

General Information

All reagents and solvents for synthesis and characterization were purchased from commercial companies and without further purification. ^{1}H-NMR and ^{13}C-NMR spectra were measured with a Switzerland Bruker DR×600 at 600 and 151 MHz using tetramethylsilane (TMS) as the internal standard. UV-vis spectra were recorded using a Hitachi U-3900 spectrometer. Photoluminescence (PL) spectra were recorded with a Horiba FluoroMax-4 spectrometer. The absolute fluorescence quantum yields (PLQY) were performed on Edinburgh Instrument FLS980 using an integrating sphere. The transient photoluminescence decay was carried out using an Edinburgh Instrument FLS980 spectrometer. Thermal gravimetric analysis was performed on a Netzsch TG 209F3 under dry nitrogen atmosphere, heating from room temperature to 800 ℃ at a rate of 10 ℃/min. Differential scanning calorimetry (DSC) was measured on DSC Q2000 at a heating rate of 10℃/min from 20 to 350℃, then cooling down to room temperature rapidly and heating up to 350℃ at a rate of 10℃/min again. Powder X-ray diffraction were recorded using Single-crystal X-ray data were collected using a Bruker APEX-II CCD diffractometer with a graphite-monochromated Mo K_{α} radiation (λ = 0.71073 Å, Bruker Corporation, Billerica, MA, USA). Molecular structures were determined by direct methods with SHELXS-97/SHELXL-97. Apart from H atoms, all other types of atoms underwent an anisotropic refinement (full-matrix least-squares on F^2). Hydrogen atoms were positioned in calculated sites having fixed isotropic thermal parameters.

These were considered in structure factor calculations at the final stage of full-matrix least-squares refinement.

The electrochemical properties were obtained via cyclic voltammetry (CV) measurement by using a CHI 660E voltammetry analyzer. Tetrabutylammoniumhexafluorophosphate ($TBAPF_6$) in anhydrous dichloromethane (0.1 M) was used as the electrolyte. A platinum wire was used as the working electrode. A platinum electrode was the counter and a calomel electrode was the reference with ferrocenium-ferrocene (Fc^+/Fc) as the internal standard. The HOMO/LUMO levels are calculated according to the following formalism:

$$E_{HOMO} = -4.8 - e(E_c^{ox} - E_f^{ox})V \quad (3)$$

where E_c^{ox} is the first oxidation peaks measured from CV curves and E_f^{ox} is the oxidation peak of ferrocene. The lowest unoccupied molecular orbital level (E_{LUMO}) was calculated from $E_{LUMO} = E_{HOMO} + E_g$, and $E_g$was estimated from the intersection of absorption and emission spectra. Theoretical simulations were performed using the Gaussian 09 package. Geometry optimization was performed by density functional theory (DFT) in B3LYP/6-31 G(d) basis sets.

OLED fabrication and characterization

OLEDs with area of 3 × 3 mm^2 were fabricated by thermal vacuum deposition onto indium tin oxide (ITO) glass substrate, which was cleaned with deionized water, acetone, and ethanol in that order. The devices' structure was ITO /MoO_3 (3 nm)/TAPC (30 nm)/TCTA (10 nm)/CBP: x wt% **TQT** (20 nm)/TmPyPb (50 nm)/LiF (1 nm)/Al (100 nm) (Device：N1, x=0 wt%, D1: x=10 wt%, D2: x=15%, D3: x=20 wt%, D4: x=30 wt%). ITO and Al are used as the anode and cathode, respectively; MoO_3 and LiF acted as the hole and electron injection layers, respectively; TAPC (4,4-cyclohexylidene bis[N, N-bis(4-methylphenyl)benzenamine]) and TCTA (tris(4-carazoyl-9-ylphenyl)amine) are served as hole-transport layer and electron blocking layer, respectively, and **TQT** doped in CBP (4,4'-Di(9H-carbazol-9-yl)-1,1'-biphenyl) is applied as emitting layer. TmPyPb (1,3,5-tri[(3-pyridyl)-phen-3-yl] benzene) is used as electron-transport materials.

The EL spectra and CIE coordinates were recorded by PR-655 spectrophotometer. The OLEDs' current density-voltage-luminance (*J-V-L*) characteristics were measured by a computer-controlled Keithley 2400 source meter integrated with a BM-70A luminance meter. The EQE was calculated from the *J-V-L* curves and spectra data. All devices were characterized without encapsulation in ambient atmosphere at room temperature.

Synthesis of TQT

5,8-dibromoquinoxaline (5.2 mmol, 1.5 g), triphenylamine-4-boronic acid (13 mmol, 3.77 g), $Pd(PPh_3)_4$） (0.26 mmol, 0.3 g) and K_2CO_3 (2 M 10 mL) were added to tetrahydrofuran (40 mL, THF). The mixed solution were stried for 3 h at 65°C. After completion of reaction, the mixture was cooled down to room temperature. Then, the organic solid were obtained by extraction using water and dichloromethane and dried with Na_2SO_4 The obtained green-yellow solid **TQT**was further purified via column chromatography using petroleum ether，PE）/DCM (2:1，V/V) with yield of 70% . ^{1}H NMR (600 MHz, $CDCl_3$) δ 8.892 (s, 2H), 7.861 (s, 2H), 7.632 (d, *J* = 1.8 Hz, 2H), 7.624 (d, *J* = 1.8 Hz, 2H), 7.313 - 7.289 (m, 8H), 7.214 (s, 4H), 7.202 (s, 6H), 7.192 (d, *J* = 2.7 Hz, 2H), 7.073 (s, 1H), 7.064 (s, 2H), 7.043 (s, 1H)。^{13}C NMR (101 MHz, $CDCl_3$-*d*) δ 147.675, 147.448, 143.957, 141.274, 139.443, 131.983, 130.007, 129.344, 124.908, 123.175, 122.609。

Five crystals, **TQT-G** (λ_{PL}= 530 nm, Φ_{PL} =81.2 %), **TQT-Y** (λ_{PL}= 575 nm, Φ_{PL} =92.7 %), **TQT-Y1** (λ_{PL}= 584 nm, Φ_{PL} =56.2 %), were obtained from THF/ethanol (1:3), THF/petroleum ether (1:3) and chloroform/ethanol (1:3) respectively. Both **TQT-O** (λ_{PL}= 593 nm, Φ_{PL} =53.4 %) and **TQT-R** (λ_{PL}= 600 nm, Φ_{PL} =24.1 %) were prepared from Chloroform-*d* ($CDCl_3$-*d*) solution, with different precipitation rates.

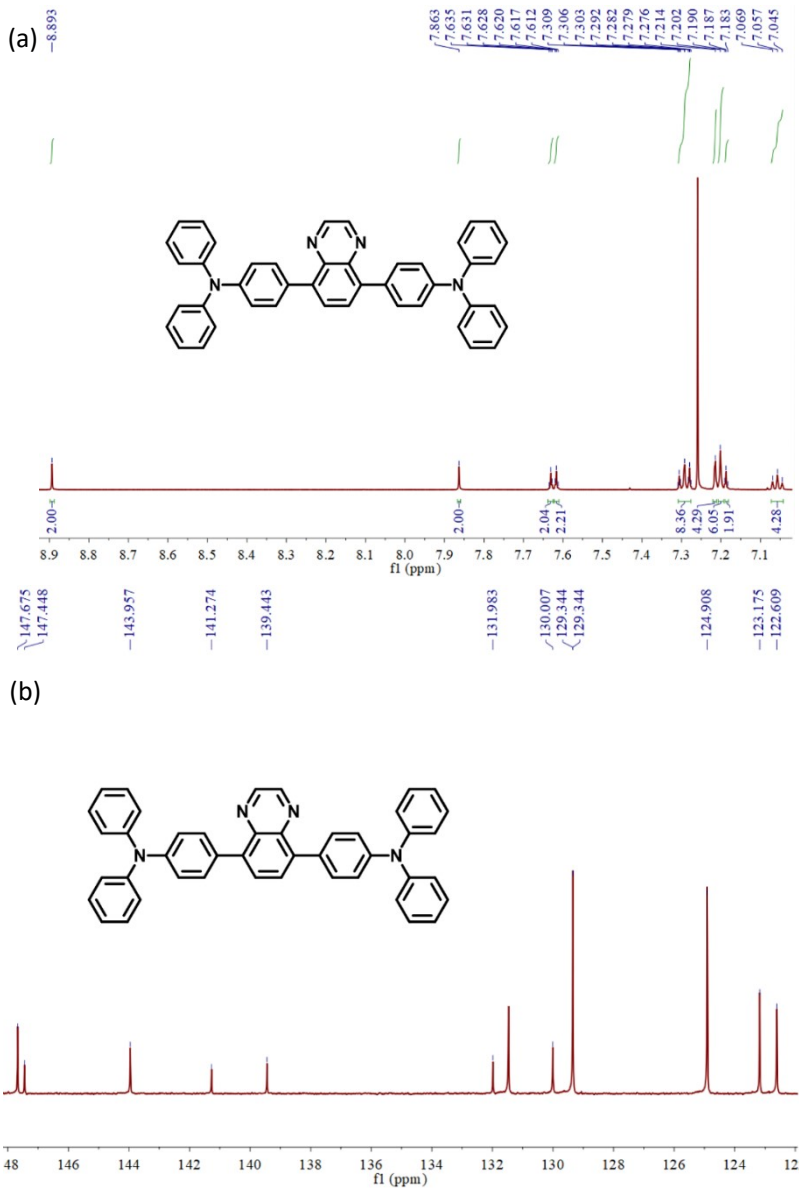

Fig. S1. ^{1}H NMR (a) and ^{13}C NMR (b) spectrum of **TQT** in $CDCl_3$

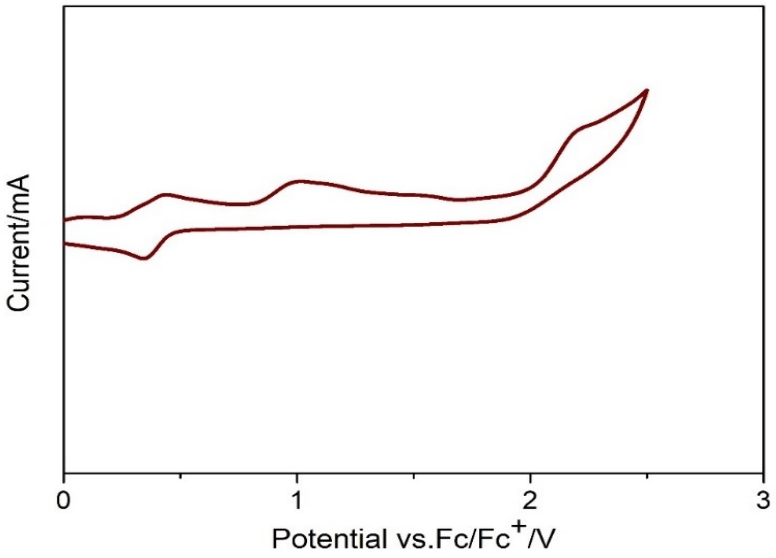

Fig. S2. Cyclic voltammogram of **TQT**

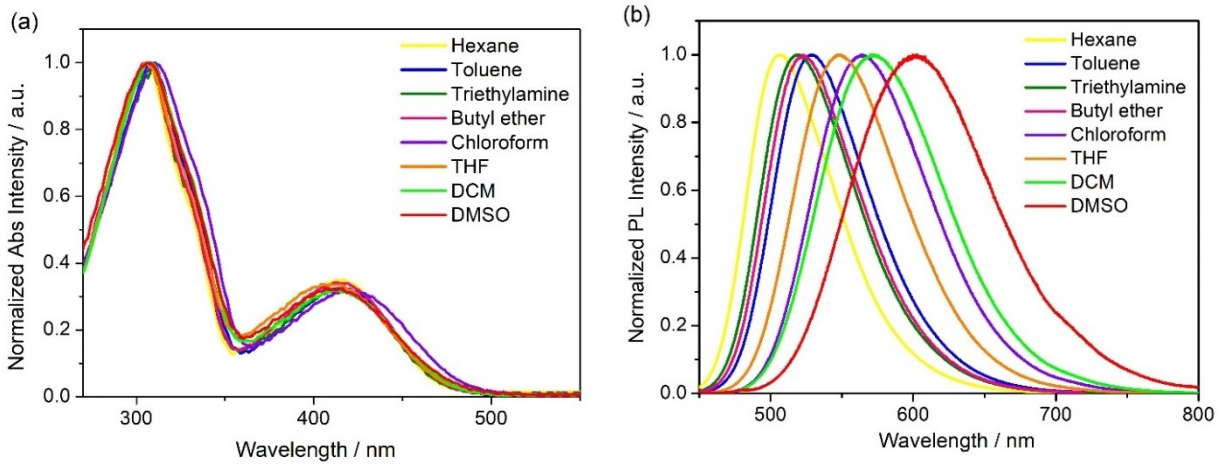

Fig. S3 Absorption and PL emission spectra of **TQT** in different solvents

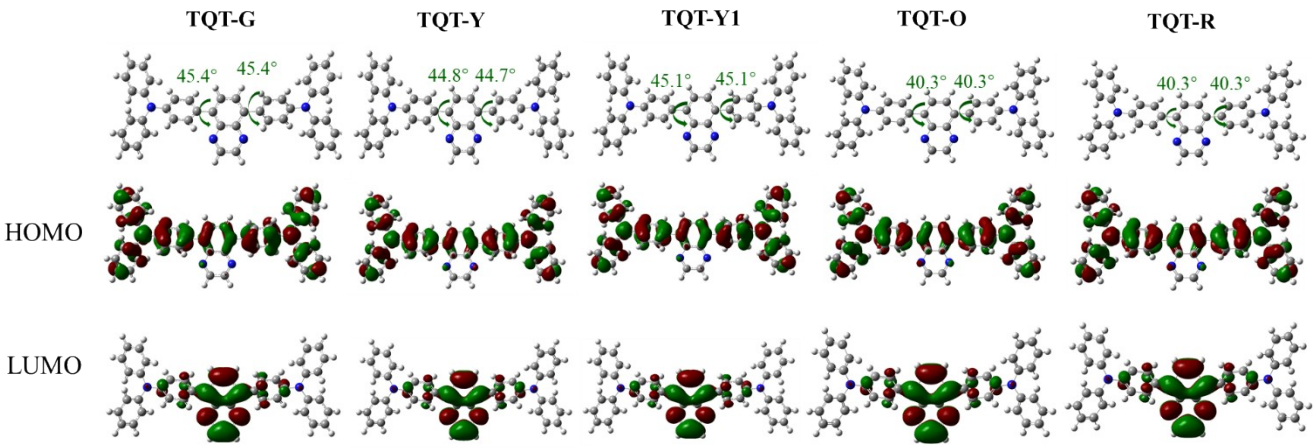

Fig. S4 Optimized molecular structures and HOMO/LUMO different **TQT** crystals

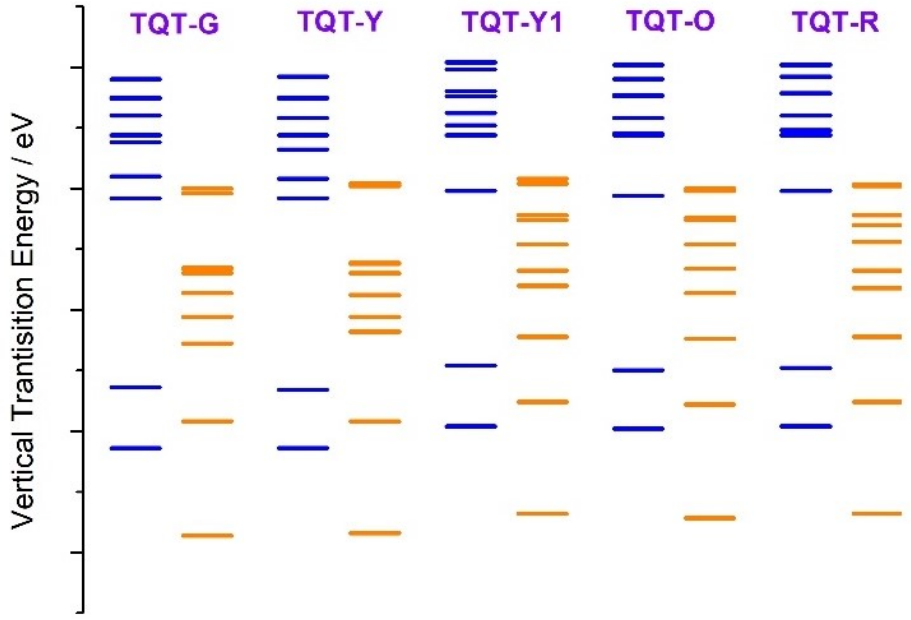

Fig.S5. The first ten singlet and triplet energy levels diagram of **TQT-G**, **TQT-Y**, **TQT-Y1**, **TQT-O** and **TQT-R** (blue line: singlet; orange line: triplet)

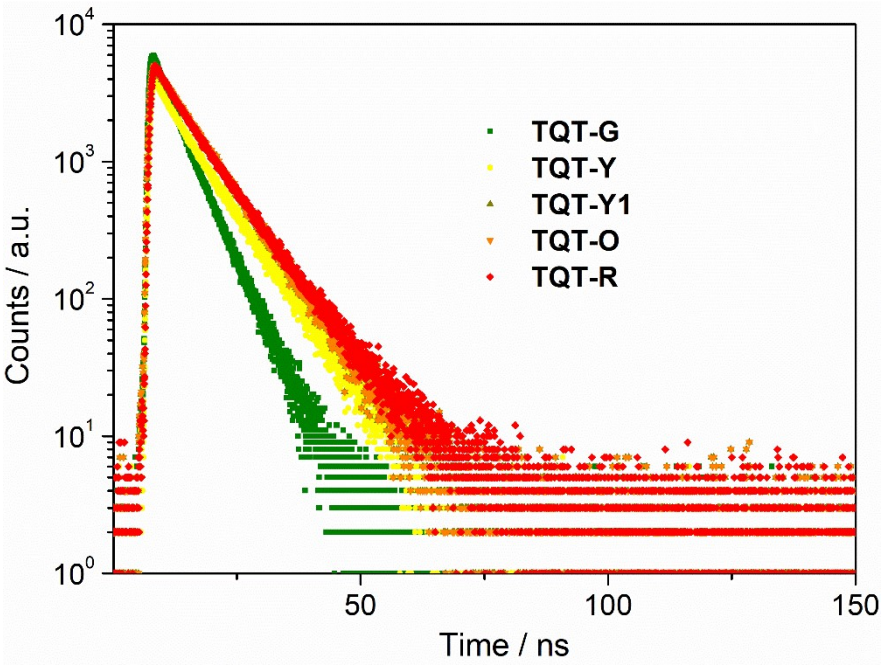

Fig. S6 fluorescent lifetime decays of five different crystals

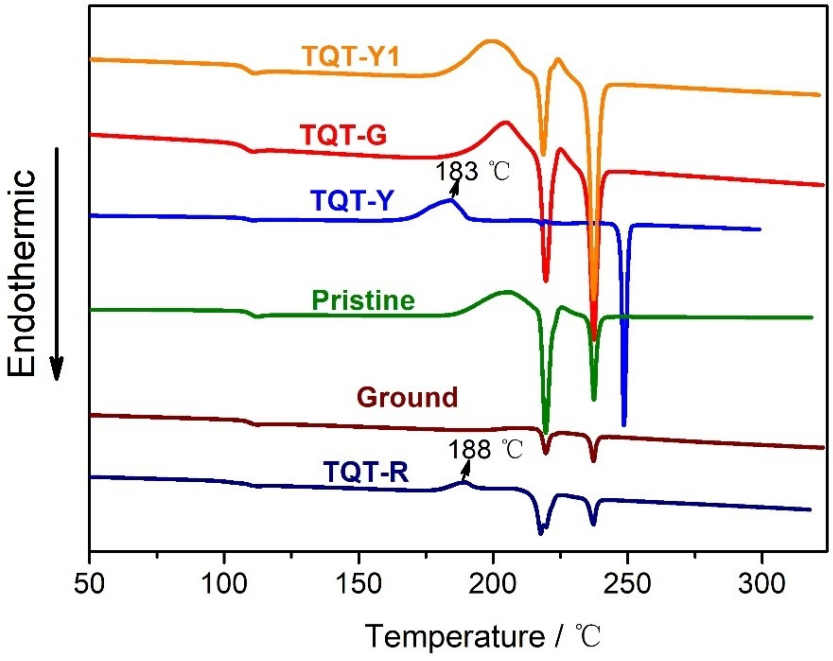

Fig. S7 DSC curves of **TQT** in different phases

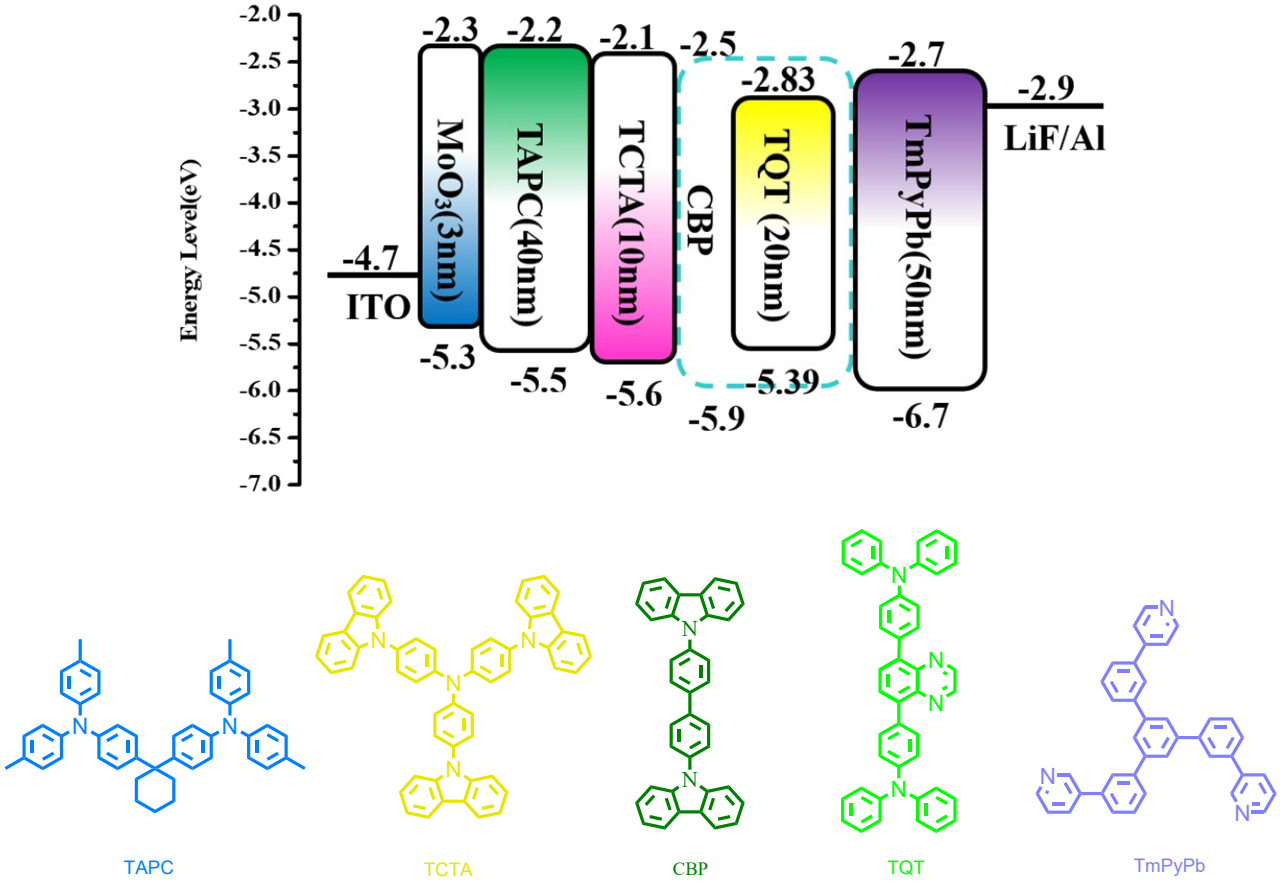

Fig. S8 Energy level diagram and molecular structural of functional materials

Table S1 The crystal data of **TQT**

Identification code	**TQT-G**	**TQT-Y**	**TQT-Y1**	**TQT-O**	**TQT-R**
Empirical formula	$C_{44}H_{32}N_4$	$C_{44}H_{32}N_4$	$C_{44}H_{32}N_4$	$C_{45.5}H_{33}Cl_{4.5}N_4$	$C_{45.5}H_{33}Cl_{4.5}N_4$
Formula weight	616.73	616.73	616.73	795.28	795.28
Temperature/K	294.10(10)	294.65	294.52	301	301
Crystal system	monoclinic	monoclinic	monoclinic	monoclinic	monoclinic
Space group	$P2_1/n$	$P2_1/c$	$P2_1/n$	$P2_1/c$	$P2_1/c$
a/ Å	10.6758(6)	16.1060(4)	10.6668(9)	16.0835(2)	16.0781(3)
b/ Å	7.6319(4)	16.8369(4)	7.6326(6)	16.8434(2)	16.8421(3)
c/ Å	40.9209(18)	16.0046(4)	40.908(2)	16.0104(2)	16.0082(3)
α /°	90	90	90	90	90
β /°	91.101	114.763(3)	91.060(6)	115.0037	115.015(2)
γ /°	90	90	90	90	90
Volume/ $Å^3$	3333.5	3941.01(19)	3330.0(4)	3930.73(11)	3928.22(12)
Z	4	4	4	4	4
ρ_{calc} / g/cm^3	1.229	1.039	1.230	1.344	1.345
μ/mm^{-1}	0.560	0.474	0.561	3.346	3.348
F(0 0 0)	1296.0	1296.0	1296.0	1642.0	1642.0
Crystal size / mm^3	0.07×0.04×0.02	0.11 × 0.07 × 0.04	0.11 × 0.09 × 0.02	0.19 × 0.15 × 0.09	0.11 × 0.07 × 0.03
2θ range for data collection/°	8.552 to139.786	8.008 to 139.592	8.53 to 139.68	6.064 to 152.956	8.044 to 152.71
Reflections collected	11268	15060	11749	303327	22929
Goodness-of-fit on F^2	1.022	1.055	1.038	1.088	1.052
Final R indexes[I≥2σ(I)]	R_1 = 0.0448, wR_2 = 0.1151	R1 = 0.0497, wR2 = 0.1422	R1 = 0.0524, wR2 = 0.1287	R_1 = 0.0804, wR_2 = 0.2425	R_1 = 0.0793, wR_2 = 0.2274
Final R indexes [all data]	R_1 = 0.0604, wR_2 = 0.1276	R1 = 0.0614, wR2 = 0.1520	R1 = 0.0756, wR2 = 0.1517	R_1 = 0.0914, wR_2 = 0.2548	R_1 = 0.0970, wR_2 = 0.2431

Table S2 Dihedral angles of **TQT** in different crystals

Single crystal	Dihedral angle			
	θ_1	θ_2	θ_3	θ_4
TQT-G	70°	37.45°	47.40°	69.03°
TQT-Y	62.70°	42.30°	45.92°	64.05°
TQT-Y1	70.13°	37.50°	47.36°	68.99°
TQT-O	41.5°	43.5°	45.99°	39.5°
TQT-R	38.9°	46.04°	43.5°	31.9°